

Electronic supplementary information

Tuning the arrangement of lamellar nanostructures: achieving dual functions of physical killing bacteria and promoting osteogenesis

Shi Mo,^{ab} Kaiwei Tang,^{bc} Qing Liao,^a Lingxia Xie,^a Yuzheng Wu,^b Guomin Wang,^b Qingdong Ruan,^b Ang Gao,^a Yuanliang Lv,^{ad} Kaiyong Cai,^e Liping Tong,^{*a} Zhengwei Wu,^{*bf} Paul K Chu,^b Huaiyu Wang^{*a}

^a *Institute of Biomedicine and Biotechnology, Shenzhen Institute of Advanced Technology, Chinese Academy of Sciences, Shenzhen, China*

^b *Department of Physics, Department of Materials Science and Engineering, and Department of Biomedical Engineering, City University of Hong Kong, Tat Chee Avenue, Kowloon, Hong Kong, China*

^c *School of Materials Science and Engineering, Xiangtan University, Xiangtan, China*

^d *School of Advanced Manufacturing, Fuzhou University, Fuzhou, China*

^e *Key Laboratory of Biorheological Science and Technology, Ministry of Education, College of Bioengineering, Chongqing University, Chongqing, China*

^f *School of Nuclear Science and Technology, University of Science and Technology of China, Hefei, China*

* E-mail: lp.tong@siat.ac.cn (L. Tong); wuzw@ustc.edu.cn (Z. Wu); hy.wang1@siat.ac.cn (H. Wang).

Contents

A. Materials and methods.....	S3
Preparation of the nanolamellar structures.....	S3
Material characterization.....	S3
<i>In vitro</i> antibacterial assays.....	S4
Bacterial morphology	S4
Bacterial interactions with different nanolamellae	S5
<i>In vitro</i> cell culture	S5-S6
Cell viability and morphology	S6
Alkaline phosphatase (ALP) assay and alizarin red staining.....	S6
Quantitative real-time polymerase chain reaction (qPCR)	S6-S7
Co-culture of bacteria and osteoblasts.....	S7
<i>In vivo</i> experiments	S7
Statistical analysis	S7
References	S8
 B. Supplementary Figures	
Figure S1-S14	S9-S22
Table S1	S23

A. Materials and methods

Preparation of the nanolamellar structures

To prepare the tilted structure, the medical grade and semi-crystalline PEEK plates (GEHR Plastics Hong Kong Ltd., China) with dimensions of $\Phi 15 \times 2$ mm were annealed ($10^\circ\text{C min}^{-1}$ to 180°C) and cooled in an argon atmosphere (denoted as P-Anneal). No annealing was performed in the preparation of the vertically aligned lamellae. The annealed and un-annealed PEEK samples were polished with 2000 and 4000 grade silicon carbide papers, ultrasonically cleaned in 96% ethanol and pure water sequentially, and dried with flowing nitrogen. For fabricating P-VL and P-TL samples, the annealed and un-annealed PEEK were then subjected to an Ar plasma treatment for 45 minutes using the AJA International, Inc. system equipped with a radio frequency source at a pressure of 1.6×10^{-2} Torr. Afterwards, the samples were cleaned in a water bath ultrasonically and then dried with flowing nitrogen. For comparison, the semi-transparent and amorphous PEEK film (Goodfellow Corporation, UK) was treated under the same conditions. To prepare the partial P-VL and P-TL samples, two regions of the PEEK substrates were shielded by silicon wafers with only the middle region exposed to the plasma as shown in Figure S4.

Material characterization

The surface topography was examined by scanning electron microscopy (SEM, XL30 FEG, Philips, Netherlands) and atomic force microscopy (AFM, NanoScope V MultiMode, Veeco, USA). The static contact angles of water or diiodomethane ($4 \mu\text{L}$) were measured by the sessile drop method on a Rame'-Hart instrument (USA) under ambient conditions and the surface energy was determined accordingly. X-ray photoelectron spectroscopy (XPS, *K-Alpha*⁺, Thermo Fisher Scientific, USA) with Al K_α excitation (72 W) and attenuated total-reflection Fourier transform infrared spectroscopy (ATR-FTIR, Frontier, PerkinElmer, USA) were employed to analyze the chemical structure. X-ray powder diffractometry (XRD, D2 Phaser, Bruker, Germany) was performed in the 2θ range from 10° to 50° and 0.02° per step and differential scanning calorimetry (DSC, 404 F3 Pegasus, Netzsch, Germany) was carried out from 30 to 400°C at a heating rate of 10°C/min . The crystalline degree was determined using the melting enthalpy ΔH_m of the samples and the ideal crystalline PEEK (130 J g^{-1}). The zeta potential was measured using 1 mM KCl solution with adjusted pH (0.05 M HCl/KOH) on an electrokinetic analyzer (Surpass3, Anton Paar, Austria).

In vitro antibacterial assays

Gram-positive *Staphylococcus aureus* (*S. aureus*) and Gram-negative *Escherichia coli* (*E. coli*) were obtained from the American Type Culture Collection (ATCC) and used in the antibacterial assays. Initially, the plate counting method was used to evaluate the antibacterial activity on the different samples. The bacteria were cultured in the Luria-Bertani (LB) medium in a shaker at 37 °C to reach an optical density at 600 nm (OD_{600}) = 0.1. After diluting 10^3 times with the sterilized physiological saline, 100 μ L of each bacteria suspension was added to the sterilized samples on a 24-well plate (NEST Biotechnology, China) and cultured for different periods of time. Subsequently, 900 μ L of the sterilized physiological saline were added to each well to elute the bacteria and 10 μ L of the bacterial eluent were added to an agar plate and incubated at 37°C for 24 hours before colony forming unit (CFU) counting. The antimicrobial efficiency was evaluated according to the following equation:

$$\text{Antimicrobial efficiency} = \frac{\text{CFU}_{\text{control}} - \text{CFU}_{\text{test}}}{\text{CFU}_{\text{control}}} \times 100\%$$

Fluorescent staining was performed to visualize the viable bacteria on the different samples. 100 μ L of the bacterial suspension (10^7 CFU mL^{-1}) were added to the samples, incubated for 6 hours, washed twice with the phosphate buffered saline (PBS, pH = 7.4), and stained by the Live/Dead BacLight bacterial viability kit (Thermo Fisher Scientific, USA) in the dark for 15 min. Afterwards, the unstained dye was rinsed with PBS three times and the viable bacteria were observed under an inverted fluorescent microscope (Axio Observer Z1, Zeiss, Germany). To assess the integrity of the bacterial membrane, the bacteria were detached from the different samples by ultrasonic elution. The detached bacteria were centrifuged at 5,000 revolutions per min (rpm) and the absorbance of the released cytoplasm in the supernatant was measured at 260 nm using an ultraviolet spectrophotometer (TU-1080PC, Persee, China).

Bacterial morphology

To analyze the morphological change on the bacteria, 100 μ L of the bacterial suspension (10^7 CFU mL^{-1}) were added to the different samples and cultured for up to 6 hours. Afterwards, the samples with bacteria were rinsed thrice with PBS, immobilized with 4% glutaraldehyde solution, dehydrated with gradient ethanol, and dried at 37 °C prior to SEM observation. In addition, 100 μ L of the bacteria media (10^9 CFU mL^{-1}) were cultured on the different samples for 6 hours, immobilized with 4% glutaraldehyde solution, and then harvested from the sample surface using a sterile surgical skin prep blade. The bacteria were immobilized again with 4%

osmium tetroxide, rinsed twice with PBS, dehydrated with gradient ethanol and acetone, embedded in epoxy resin, and sliced into thin sections. After uranyl acetate staining, the sections were loaded on a copper mesh and observed by transmission electron microscopy (TEM, H-7650, Hitachi, Japan).

Bacterial interactions with different nanolamellae

To determine bacterial chemotaxis and selective adhesion on the samples, the PEEK substrates partially modified (constructed with P-VL/P-TL nanolamellae or plasma-treated for 5 min) were cultured with *E. coli* and *S. aureus* for 6 hours, respectively. The samples were rinsed gently with PBS twice, fixed with 4% paraformaldehyde, stained by the Gram stain kit (BKMAN, China), and observed by optical microscopy (BX53M, Olympus, Japan). During the test for bacterial adhesion, a part of the partial P-TL and Ar-5 samples with bacteria were rinsed with the PBS buffer using a parallel-placed syringe. The zeta potential was measured on the Zetasizer Nano ZS (Malvern, UK) after ultrasonically collecting the attached bacteria from the samples. To analyze the other interaction factors, molecular dynamic simulation was performed on the simulated bacterial membrane composed of a mixture of palmitoyloleoyl-phosphatidylethanolamine and palmitoyloleoylphosphatidylglycerol (3:1 ratio) and PEEK nanoplates as the models. The martini coarse grain force field, one of the commonly used and extensively validated force field and periodic boundary conditions, was adopted in the computation¹. The PEEK nanoplates with different orientations ($\theta = 90^\circ$ or 30°) were put under the simulated bacterial membrane and a time duration of 60 ns with a coupling constant of 2 fs was applied to the isothermal-isochoric ensemble. In the simulation, the temperature was maintained at 298.15 K by the Berendsen method with the coupling constant of 1.0 ps². In each run, the SHAKE algorithm and particle mesh Ewald method were used to determine the bond lengths and long-range electrostatic interactions, respectively. A 20 Å cut-off was used for the van der Waals forces and Coulomb interactions and the simulation was performed using the Groningen Machine for Chemical Simulation (GROMACS)³. The generated trajectories were evaluated by the GROMACS inbuilt tools and the results were visualized using visual molecular dynamics⁴.

In vitro cell culture

The osteoblasts (MC3T3-E1 cells) obtained from ATCC were cultured with Dulbecco's modified eagle medium (DMEM, Hyclone, USA) containing 10% fetal bovine serum (FBS, Gibco, USA) in an incubator at 37 °C under 5% CO₂, and 90% moisture. Before the experiments, the cells were detached from the culture dishes, centrifuged (1200 rpm, 5 min), and diluted to about 2×10^4 cells mL⁻¹ with the fresh medium. In osteogenic induction, the

culture medium was supplemented with 50 µg/ml ascorbic acid, 10 mM β-glycerophosphate and 100 nM dexamethasone.

Cell viability and morphology

1 mL of the cell suspension (2×10^4 cells mL⁻¹) were added to each sample on the 24-well plate and incubated for 1, 3 and 7 days. At each time point, the culture medium was replaced with DMEM containing 10% 3-(4,5-dimethylthiazol-2-yl)-2,5-diphenyltetrazolium bromide and incubated for another 4 hours for formazan formation. Subsequently, the formazan product was dissolved by dimethyl sulfoxide and the absorbance at 570 nm was measured. Cell apoptosis/necrosis was analyzed by using the Annexin V-FITC/PI assay kit (Beyotime, China) and a flow cytometer (CytoFLEX, Beckman Coulter, USA). Briefly, 1 mL of the cell suspension with a density of 5×10^4 cells mL⁻¹ was added to each sample and incubated for 1 and 3 days, respectively. Afterwards, the cells on each sample were harvested and stained with FITC and PI following the manufacturer's instructions, and finally analyzed by flow cytometry. Before examining the cell morphology by SEM (SEM, XL30 FEG, Philips, Netherlands), the cells were cultured for 1 day, rinsed twice with PBS, immobilized with 4% glutaraldehyde solution, dehydrated with gradient ethanol, dried at 37 °C and sputtered with platinum.

Alkaline phosphatase (ALP) assay and alizarin red staining

After osteogenic induction for 7 and 14 days, the cells in the different groups were treated with the cell lysis buffer (Beyotime, China) and the ALP activity and total intracellular protein were determined using the ALP Assay Kit (Beyotime, China) and BCA Protein Assay Kit (Beyotime, China), respectively. The ALP activity was normalized to the total protein content and quantitatively presented as nmol/min/mg protein. The degree of mineralization was evaluated by alizarin red staining. After osteogenic induction of osteoblasts on different samples for 14 days, the attached cells were washed three times with PBS, fixed in 75% ethanol for 1 hour, and stained with 1% alizarin red solution (pH 4.2, Solarbio, China) for 10 min. Afterwards, the unbound dye was removed by flushing with water and the stained samples were observed using a stereoscopic microscope (Stemi SV11, Zeiss, Germany). In the semi-quantitative analysis, the bound stain was eluted with 10% acetic acid and the absorbance at 405 nm was monitored by a microplate reader (Multimode microplate reader, Bio Tek, USA).

Quantitative real-time polymerase chain reaction (qPCR)

After osteogenic induction for 14 and 21 days, the total RNA was extracted from the cells in different groups by adding Trizol reagent (Invitrogen, USA). The complementary DNA (cDNA) was synthesized from 1000 ng of total RNA using a PrimeScript RT Master Mix kit (TaKaRa, Japan) following the manufacturer's instructions. The expressions of osteogenic

genes including ALP, osteocalcin (OCN), and osteopontin (OPN) were quantitatively analyzed by performing qPCR on a CFX96 detection system (BioRad, USA) using a mixture of TransStart Green qPCR SuperMix UDG Kit (TransGen Biotech, China). β -actin was selected as the housekeeping gene and the $2^{-\Delta\Delta C_t}$ method was employed to calculate the relative gene expression levels. The target genes (ALP, OCN, OPN and β -actin) and corresponding primer sequences are listed in Table S1.

Co-culture of bacteria and osteoblasts

For co-culturing bacteria and osteoblasts on different samples, 100 μ L of the bacterial suspension (10^5 CFU mL^{-1}) was initially added to each sample on the 24-well plate and cultured for 3 hours. Afterwards, each sample was rinsed twice with PBS, and then 1 mL of the cell suspension (2×10^4 cells mL^{-1}) was added. After 1 day of co-culture, each sample was rinsed twice with PBS, immobilized with 4% glutaraldehyde solution, dehydrated with gradient ethanol, dried at 37 °C, sputtered with platinum and observed by SEM (Phenom Pro G6, Thermo Scientific, China). After 1 and 3 days of co-culture, each sample was rinsed twice with PBS, immobilized with 4% glutaraldehyde solution, stained for the cell nuclei with 5 $\mu\text{g}/\text{mL}$ Hoechst 33342 (Yeasen Biotechnology, Shanghai, China) and examined by fluorescent microscopy (BX53, Olympus, Japan).

In vivo experiments

The animal experiments were approved by the Ethics Committee for Animal Research of Shenzhen Institutes of Advanced Technology, Chinese Academy of Sciences. 12-week-old male Sprague Dawley (SD) rats with weight of 250-300 g were maintained under specific pathogen free conditions and used in the following *in vivo* experiments for 6 rats in each group. To evaluate the anti-infective performance *in vivo*, 100 μ L of the *E. coli* solution (10^6 CFU mL^{-1}) were seeded onto the samples (pristine PEEK, P-VL and P-TL) with dimensions of $\Phi 10 \times 1$ mm and cultured for 1 hour. Afterwards, the contaminated samples were subcutaneously implanted into the two backsides of the depilated rats and the incisions were carefully closed. After 7 days, the rats were sacrificed and the specimens were harvested and H&E staining was performed to evaluate the inflammatory response of the peri-implant tissues. In the osteogenesis assessment, a horizontal defect (2 mm in diameter) was drilled in the tibia in the back-legs of each rat and the implants were inserted into the openings. The experimental rats were sacrificed after 8 weeks and the femurs containing the implants were harvested and fixed in paraformaldehyde. The peri-implant newly formed bone was imaged by micro-CT (SkyScan 1176, Bruker, Germany) and the 3D images were reconstructed using the NRecon software (Skyscan) and CTvol program (SkyScan). A hollow cylinder with a thickness of 50 μm from

the implant surface and length of 6 mm of the implant was defined as the volume of interest. Qualitative analyses of bone volume/total volume (BV/TV) and trabecular number (Tb.N) are more substantial on P-TL with a relatively low trabecular separation (Tb.Sp) conducted by 3D bone morphometric analysis. The fixed tissue and implant were decalcified in ethylenediaminetetraacetic acid for 1 month and embedded in paraffin to prepare the bone tissue sections. Finally, the thin sections were stained with Van Gieson and hematoxylin and eosin (H&E) to assess peri-implant bone regeneration. To observe the bone-implant interfaces, Van Gieson staining was carried out on the longitudinal slices prepared from the un-decalcified samples.

Statistical analysis

The experiments were performed at least in triplicate. The data were analyzed by the one-way ANOVA and shown as mean \pm stand deviation (SD). A difference of $*p < 0.05$ was considered to be significant and that of $**p < 0.01$ or $***p < 0.001$ was considered to be highly significant.

References

- 1 S. J. Marrink, H. J. Risselada, S. Yefimov, D. P. Tieleman and A. H. de Vries, *J. Phys. Chem. B*, 2007, **111**, 7812–7824.
- 2 H. J. C. Berendsen, J. P. M. Postma, W. F. van Gunsteren, A. DiNola and J. R. Haak, *J. Chem. Phys.*, 1984, **81**, 3684–3690.
- 3 M. J. Abraham, T. Murtola, R. Schulz, S. Páll, J. C. Smith, B. Hess and E. Lindahl, *SoftwareX*, 2015, **1–2**, 19–25.
- 4 W. Humphrey, A. Dalke and K. Schulten, *J. Mol. Graph.*, 1996, **14**, 33–38.

B. Supplementary Figures

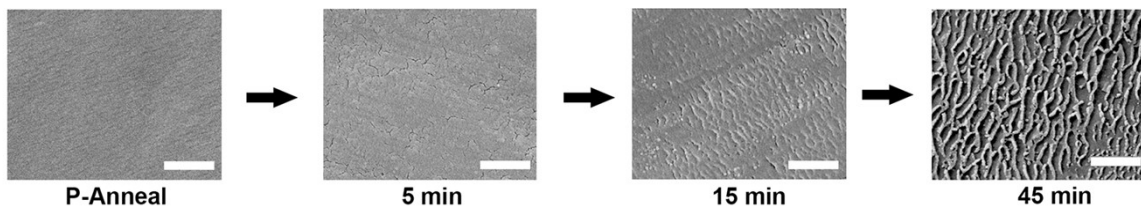


Fig. S1. Formation of the nanolamellar structure on the annealed PEEK as the argon plasma treatment is increased (scale bar = 500 nm).

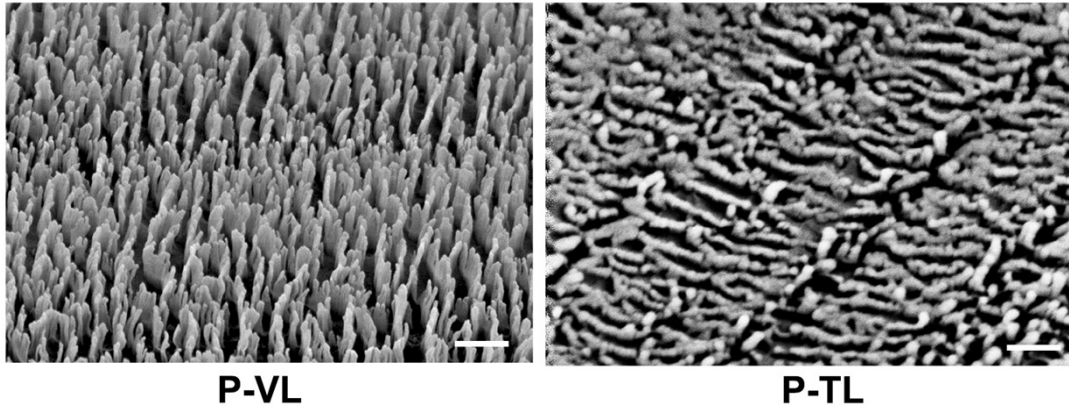
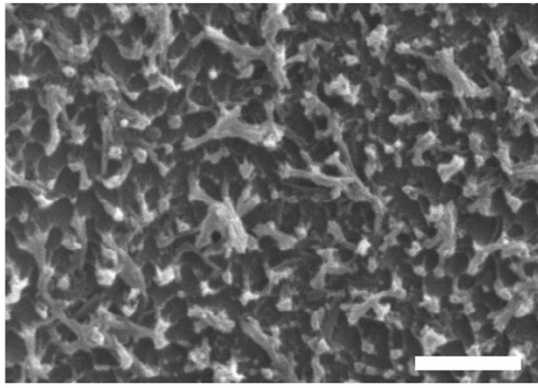
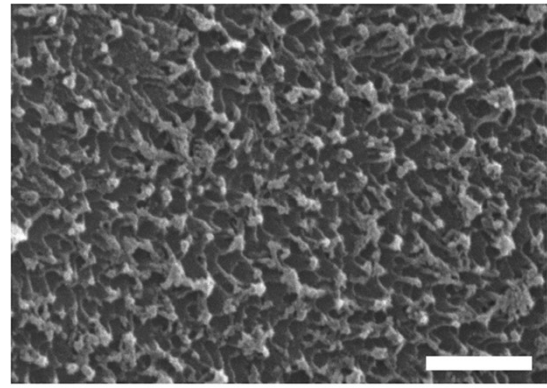


Fig. S2. The SEM images of PV-L and PT-L observed from side view at an angle of 45° (scale bar = 200 nm).



N-PEEK



O-PEEK

Fig. S3. SEM images of the nano-morphology on PEEK after treatment with the nitrogen plasma (N-PEEK) and oxygen plasma (O-PEEK) using the same parameters as the Ar plasma treatment (scale bar = 500 nm).

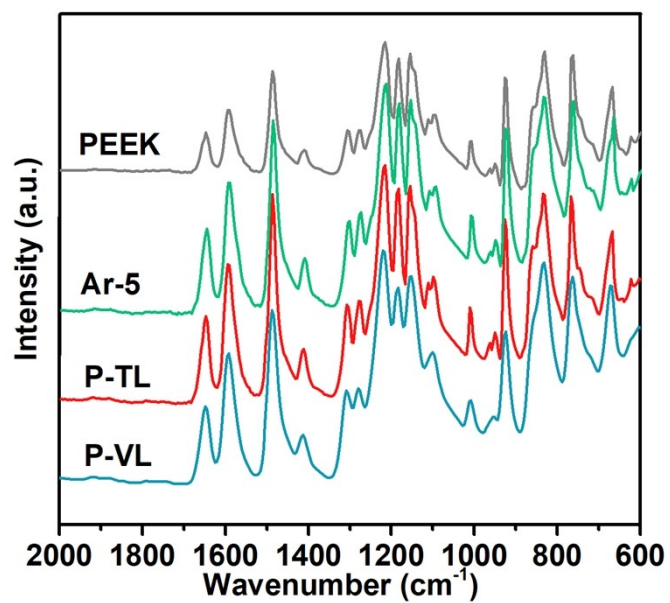


Fig. S4. ATR-FTIR spectra acquired from the different samples showing the absence of new functional groups after the Ar plasma treatment.

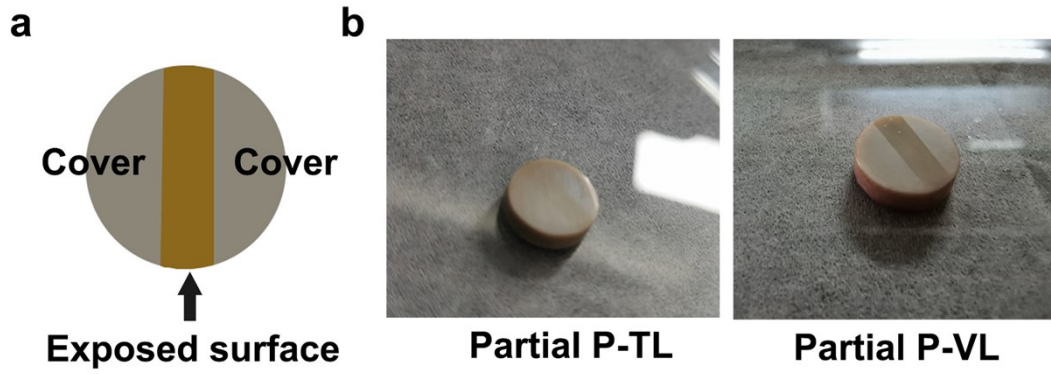


Fig. S5. (a) Illustration of the preparation of the partial P-TL and partial P-VL samples: Two regions of the substrates are shielded by silicon wafers and a middle region is exposed to the Ar plasma. (b) Pictures of the partial P-TL and partial P-VL samples showing different reflections from the middle regions.

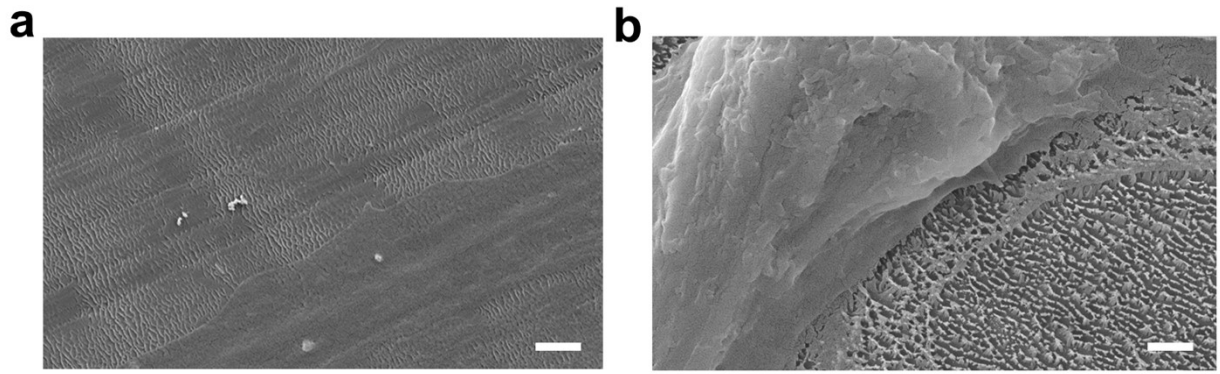


Fig. S6. SEM images showing the behavior of osteoblasts on (a) P-TL and (b) P-VL (scale bar = 1 μm).

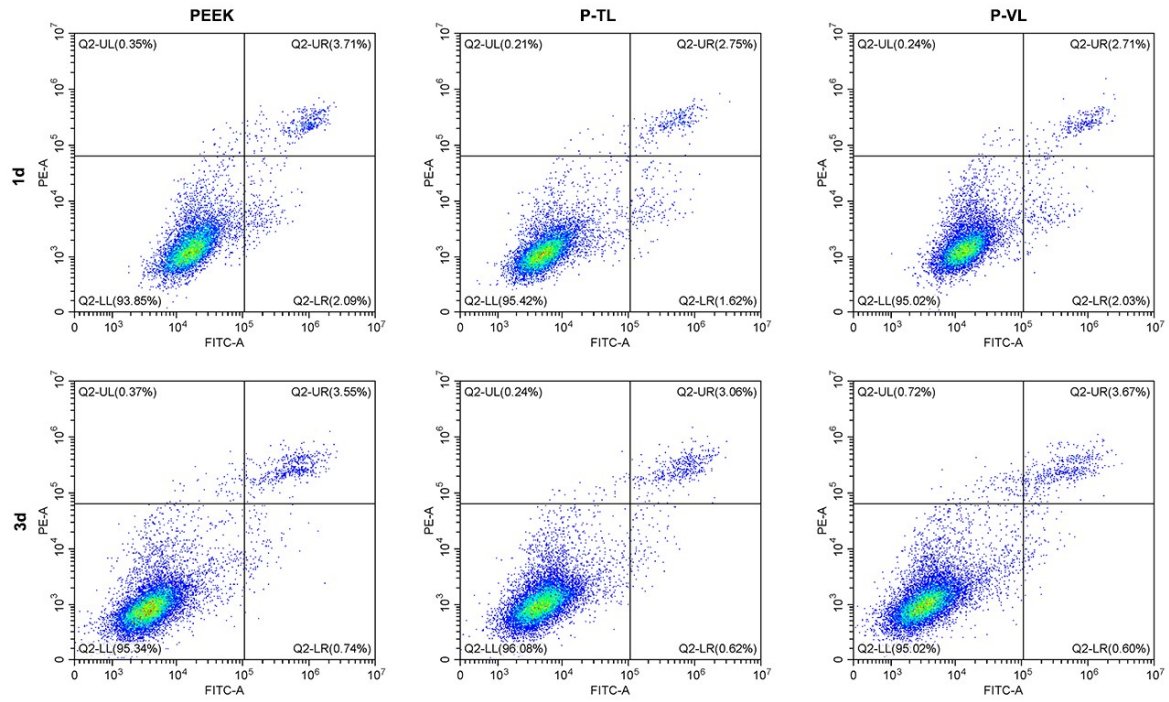


Fig. S7. Flow cytometry analysis (cell apoptosis and necrosis) of osteoblasts cultured on different samples for 1 and 3 days.

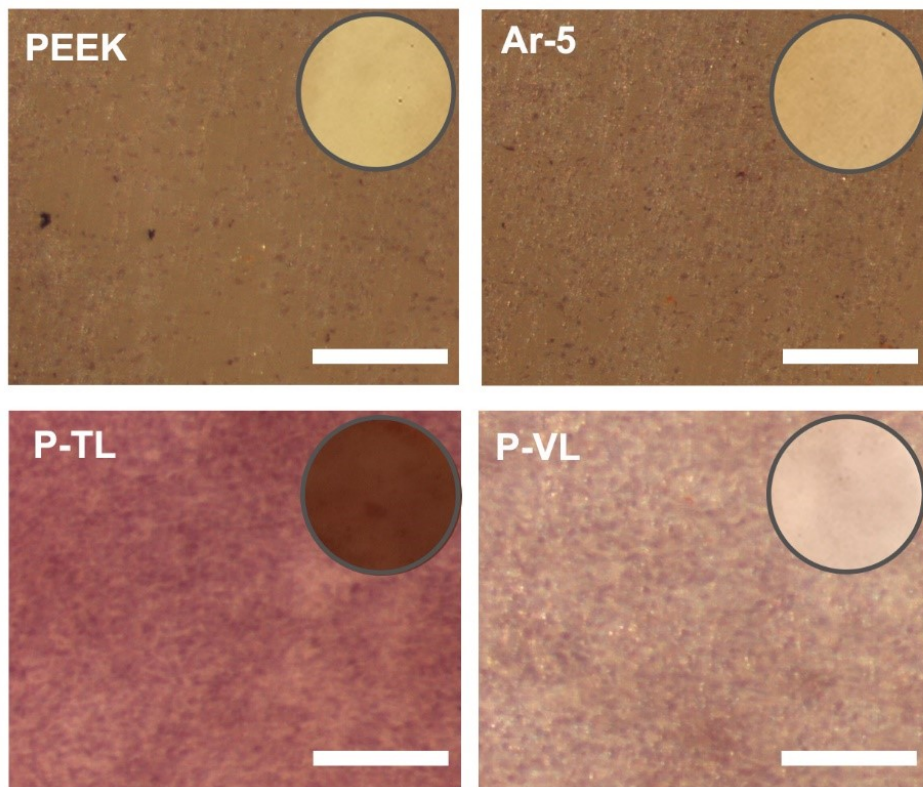


Fig. S8. Images showing mineralization of osteoblasts on the different samples after osteogenic induction for 14 days with the large-area images shown in the insets on the top-right (scale bar = 500 μm).

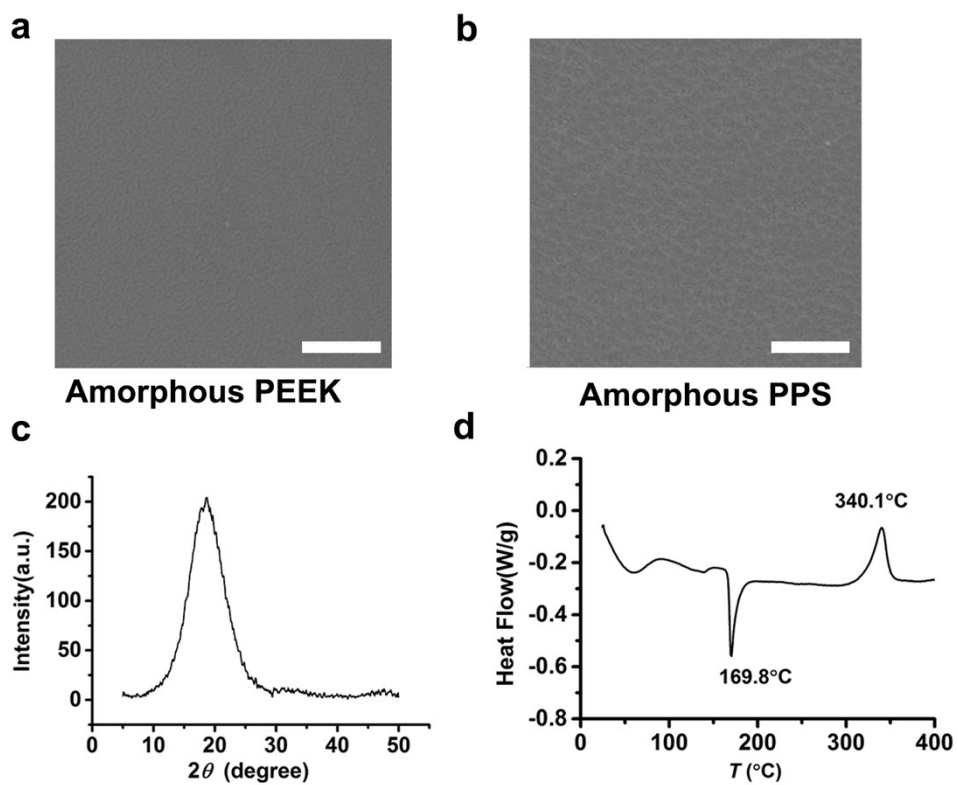


Fig. S9. SEM images of (a) Amorphous PEEK, (b) PPS after the Ar plasma treatment (scale bar = 500 nm); (c) XRD spectrum of PEEK; (d) DSC curve of PPS.

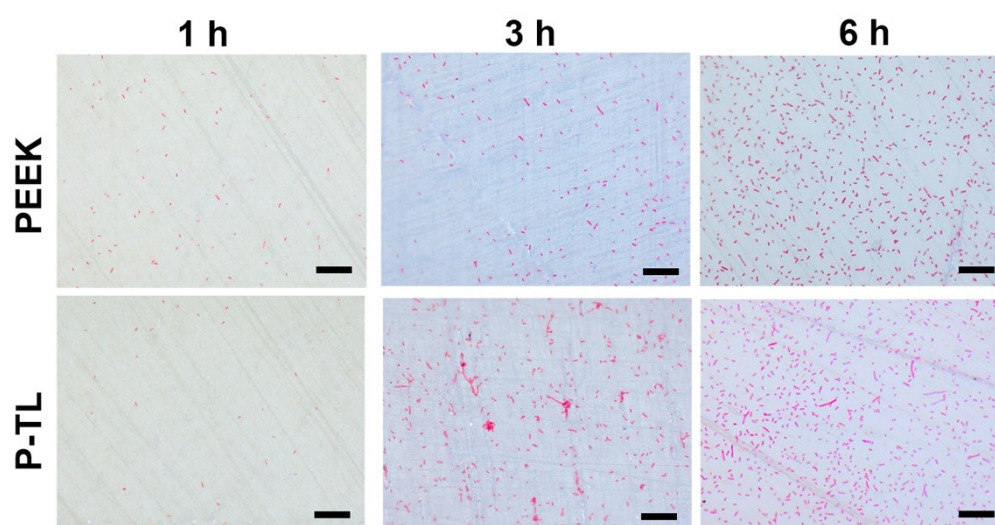


Fig. S10. Gram staining images of *E. coli* on PEEK and P-TL after incubation for 1, 3 and 6 hours (scale bar = 20 μm).

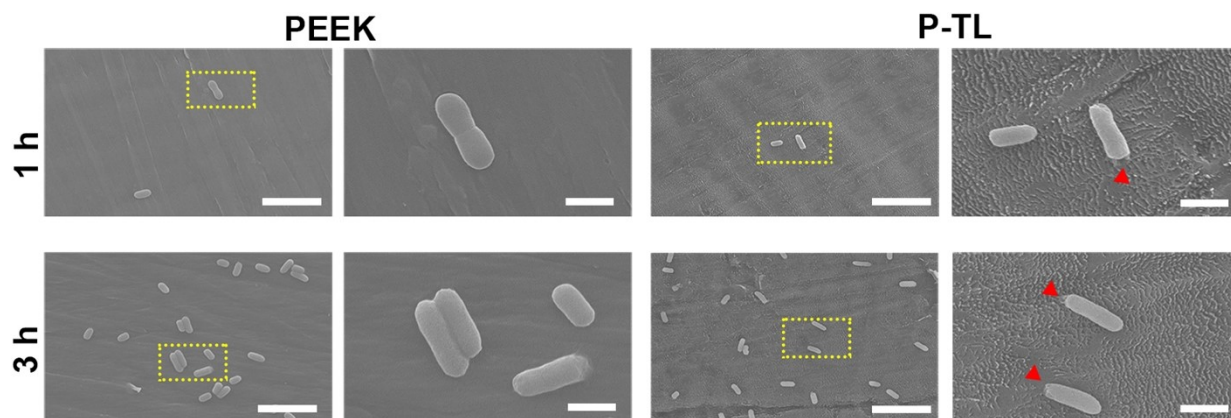


Fig. S11. SEM images of *E. coli* on PEEK and P-TL after incubation for 1 and 3 hours with the red triangles indicating defects at the poles of the cultured bacteria due to the initial destructive effect [scale bar (left column) = 5 μm ; scale bar (right column) = 1 μm].

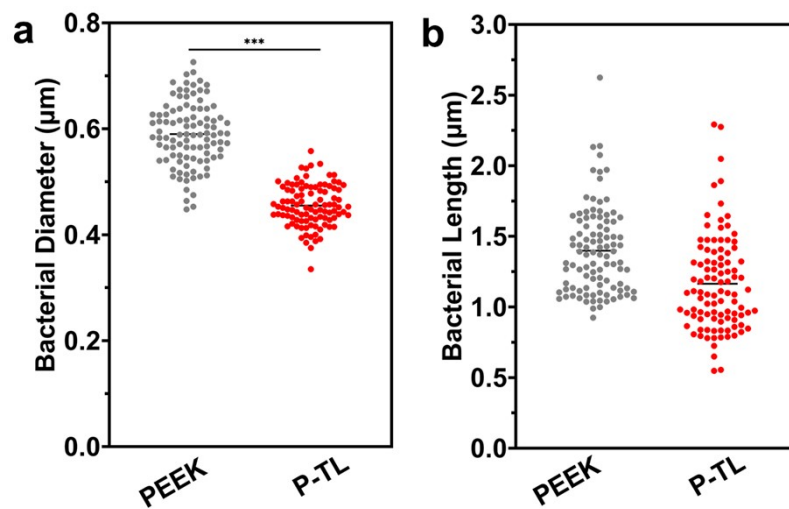


Fig. S12. (a) Diameters and (b) Lengths of *E. coli* on PEEK and P-TL after incubation for 3 hours with the bacteria size measured by ImageJ software. *** $p < 0.001$ was considered to be highly significant.

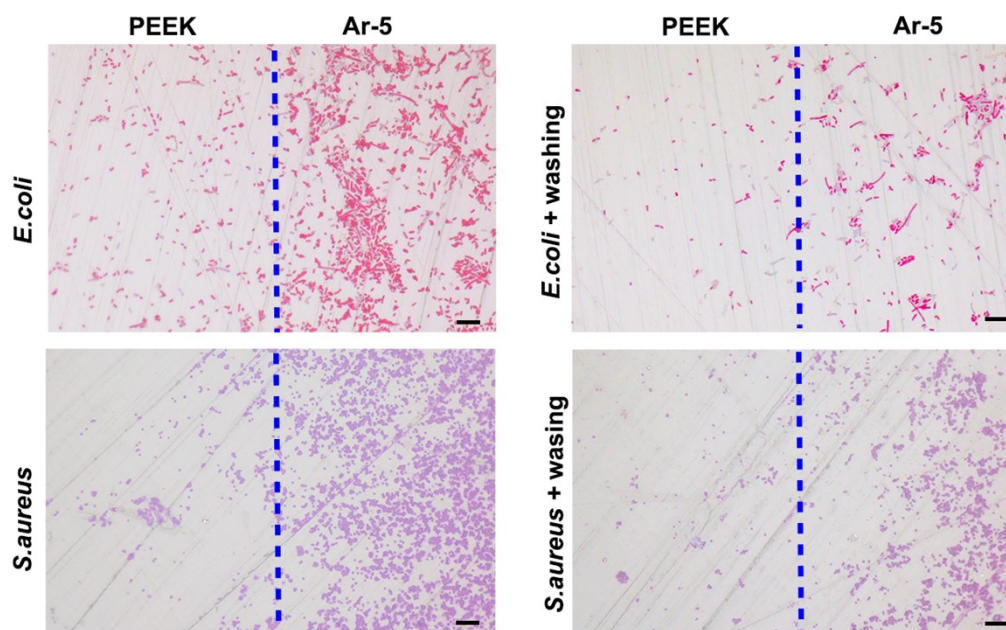


Fig. S13. Gram staining images of *E. coli* and *S. aureus* attached to the partial Ar-5 samples before and after PBS washing (scale bar = 10 μm). The blue line represents the boundary between the PEEK regions (left) and Ar-5 regions (right).

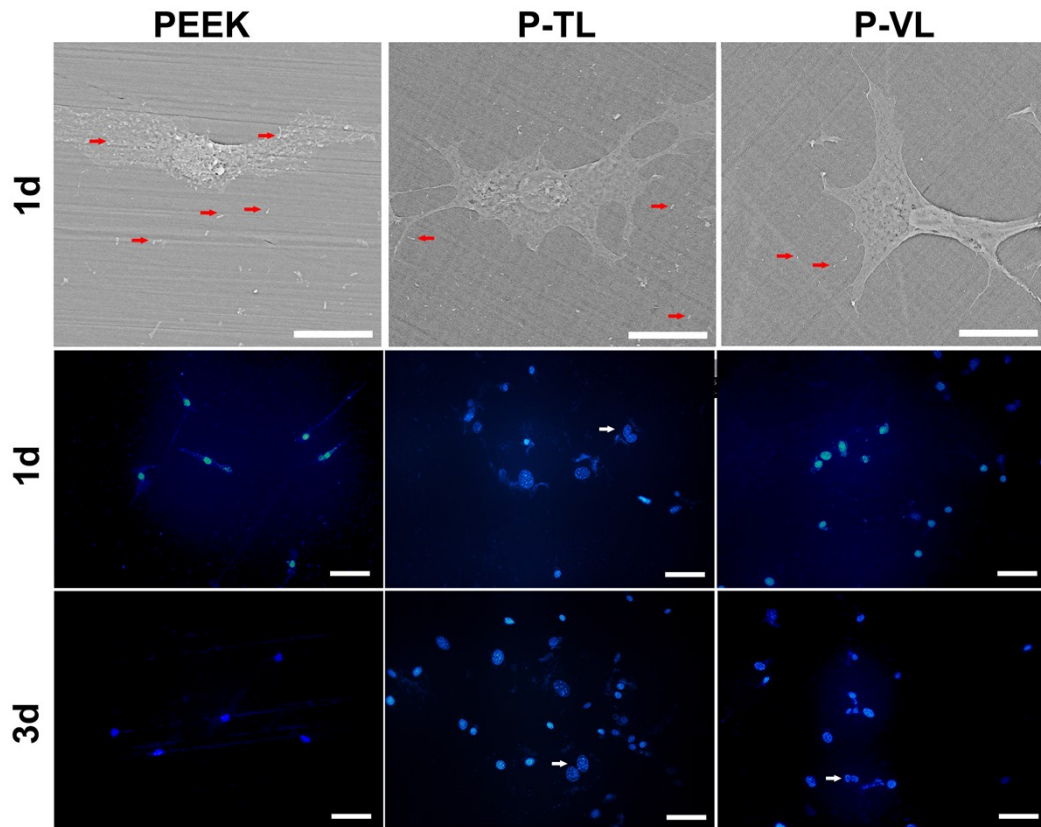


Fig. S14. (a) SEM images of bacteria and osteoblasts co-cultured on different samples for 1 day, red arrows indicate the presence of bacteria (scale bar = 20 μm). (b) Fluorescent staining images of bacteria and osteoblasts co-cultured on different samples for 1 and 3 days, white arrows indicate the growth and division of osteoblasts (scale bar = 50 μm).

Table S1. Primer sequences for the qPCR analysis.

Primers	Sequences (5'-3')
β-actin	Forward: CGTAAAGACCTCTATGCCAACA
	Reverse: AGCCACCAATCCACACAGAG
ALP	Forward: TCAGAAGCTAACACCAACG
	Reverse: TTGTACGTCTTGGAGAGGGC
OCN	Forward: GCAAAGGTGCAGCCTTTGTG
	Reverse: GGCTCCCAGCCATTGATACAG
OPN	Forward: TCACCTGTGCCATACCAGTTAA
	Reverse: GGCTCCCAGCCATTGATACAG